Glacial cold-water coral growth in the Gulf of Cádiz: Implications of increased palaeo-productivity

Claudia Wienberg, Norbert Frank, Kenneth Mertens, Jan-Berend Stuut, Margarita Marchant, Jan Fietzke, Furu Mienis, Dierk Hebbeln

Glacial cold-water coral growth in the Gulf of Cádiz: Implications of increased palaeo-productivity

Claudia Wienberg[a,*], Norbert Frank[b], Kenneth N. Mertens[c], Jan-Berend Stuut[d,a], Margarita Marchant[e], Jan Fietzke[f], Furu Mienis[a,d], Dierk Hebbeln[a]

[a] *Center for Marine Environmental Sciences (MARUM), University of Bremen, Leobener Str., 28359 Bremen, Germany*

[b] *Laboratoire des Sciences du Climat et de l'Environnement (LSCE), Bât.12, Avenue de la Terrasse, F-91198 Gif-sur-Yvette, France*

[c] *Research Unit Palaeontology (RUP), Ghent University, Krijgslaan 281 S8, 9000 Ghent, Belgium*

[d] *Royal Netherlands Institute for Sea Research (NIOZ), Landsdiep 4, 1797 SZ t'Horntje (Texel), The Netherlands*

[e] *Departamento de Zoología, Facultad de Ciencias Naturales y Oceanográficas, Universidad de Concepción, Casilla 160-C, Concepción, Chile*

[f] *Leibniz-Institute of Marine Sciences, IFM-GEOMAR, Wischhofstr. 1-3, 24148 Kiel, Germany*

* *Corresponding author. Tel: +49 421 21865652; Fax: +49 421 2189865652*
E-mail address: cwberg@marum.de (C. Wienberg)

ABSTRACT

A set of 40 Uranium-series datings obtained on the reef-forming scleractinian cold-water corals *Lophelia pertusa* and *Madrepora oculata* revealed that during the past 400 kyr their occurrence in the Gulf of Cádiz (GoC) was almost exclusively restricted to glacial periods. This result strengthens the outcomes of former studies that coral growth in the temperate NE Atlantic encompassing the French, Iberian and Moroccan margins dominated during glacial periods, whereas in the higher latitudes (Irish and Norwegian margins) extended coral growth prevailed during interglacial periods. Thus it appears that the biogeographical limits for sustained cold-water coral growth along the NE Atlantic margin are strongly related to climate change. By focussing on the last glacial-interglacial cycle, this study shows that palaeo-productivity was increased during the last glacial. This was likely driven by the fertilisation effect of an increased input of aeolian dust and locally intensified upwelling. After the Younger Dryas cold event, the input of aeolian dust and productivity significantly decreased concurrent with an increase in water temperatures in the GoC. This primarily resulted in reduced food availability and caused a widespread demise of the formerly thriving coral ecosystems. Moreover, these climate induced changes most likely caused a latitudinal shift of areas with optimum coral growth conditions towards the northern NE Atlantic where more suitable environmental conditions established with the onset of the Holocene.

Keywords: cold-water corals; last glacial; productivity; aeolian dust; Gulf of Cádiz; NE Atlantic

1. Introduction

Along the NE Atlantic margin cold-water corals occur in a belt that extends from northern Norway (Barents Sea, 70°N; Lindberg et al., 2007) down to NW Africa (off Mauritania, 16°N; Colman et al., 2005). These ecosystems vary strongly with respect to their appearance,

structure and coral vitality. Large flourishing *Lophelia*-reefs occur along the Norwegian margin. With a horizontal dimension of several hundred meters to kilometres they developed to the largest known living cold-water coral reefs worldwide (Fosså et al., 2005). Along the Irish margin cold-water corals are associated with coral mounds that vary in height from a few metres up to 380 m being often densely covered by living coral colonies (Wheeler et al., 2007, and refs. therein). Further to the south, cold-water corals mainly occur as isolated colonies or accumulations of fossil corals in the Bay of Biscay (Reveillaud et al., 2008), on seamounts (Duineveld et al., 2004) and within canyons along the Iberian margin (Tyler et al., 2009), and on coral mounds along the NW African margin (Wienberg et al., 2009).

Along with the geographic distribution, a distinct stratigraphic pattern regarding the development of cold-water coral ecosystems along the NE Atlantic margin has been observed during the last glacial-interglacial cycle. Reefs of Holocene age on the Norwegian shelf started to develop after the retreat of glaciers at the termination of the last glacial (Freiwald et al., 2004). The Irish coral mounds seem to be restricted to interglacials with a very few exceptions (Dorschel et al., 2005; Eisele et al., 2008) and the latest re-establishment of cold-water coral ecosystems appears to have been started after the Younger Dryas (YD) cold reversal (Frank et al., 2009). To the south along the French, Iberian and Moroccan margins, corals are suggested to have been widely distributed during the last glacial (Schröder-Ritzrau et al., 2005; Wienberg et al., 2009). In actual fact, although the Gulf of Cádiz (GoC) was recently identified to be an important cold-water coral site in the temperate NE Atlantic, this area is at present mainly characterised by so-called 'coral graveyards' with only very few living corals (Foubert et al., 2008; Wienberg et al., 2009). Such current depauperation of live coral ecosystems might be explained by the recent warm and oligotrophic conditions in the GoC forcing reduced food availability (Wienberg et al., 2009). In addition, tidal currents and internal waves that have been identified to be

54 important hydrodynamic processes for supplying food particles to and through the coral
55 thickets (White et al., 2005; White et al., 2007) nowadays do not seem to play a major role
56 in the GoC (Wienberg et al., 2009). However, the widespread occurrence of fossil corals
57 suggests more favourable oceanographic conditions in the past. Indeed, initial datings
58 revealed that cold-water corals have been common in the GoC during the last glacial
59 (Wienberg et al., 2009).
60
61 The present study aims to refine and extend this observed stratigraphic pattern of coral
62 occurrence along the NE Atlantic margin by 40 Uranium-series datings of reef-forming
63 scleractinian cold-water corals from sediment cores retrieved in various areas of the GoC.
64 Moreover, it is intended to relate the prosperity and/or demise of cold-water corals in the GoC
65 to a distinct environmental and oceanographic setting that altered along with climate change.
66 Thus, we aim to identify the main forcing factors triggering the development of cold-water coral
67 ecosystems in the GoC.
68
69 **2. Regional setting**
70 The GoC is situated west of the Strait of Gibraltar, and thus connects the open North Atlantic
71 Ocean and the Mediterranean Sea (Fig. 1). It is bordered by the Iberian Peninsula and the NW
72 African coasts and extends from Cape St. Vincent at the southwestern tip of Portugal down to
73 the Moroccan Atlantic margin at 33°N (Mauritzen et al., 2001). The Iberian continental shelf
74 widens from ~15 km west of Faro to ~50 km further to the east (Garcia-Lafuente and Ruiz,
75 2007), which is similar to the width of the Moroccan shelf (<60 km; Mittelstaedt, 1991).
76
77 The deeper basin of the GoC is characterised by a widespread occurrence of diapiric ridges
78 and mud volcanoes (Somoza et al., 2003). Many of these mud volcanoes were identified to
79 be covered by fossil cold-water corals (Somoza et al., 2003; Wienberg et al., 2009). Further
80 conspicuous topographic features in the GoC are hundreds of coral mounds that are 20-30

m in height, and 50-200 m in length, and that are covered by fossil corals. They are restricted to the Moroccan margin where they have been found in a water depth between 400 and 960 m (Foubert et al., 2008; Hebbeln et al., 2008; Wienberg et al., 2009). The coral mounds are mainly arranged as clusters and are situated amidst mud volcanoes and on top of diapiric ridges. Detailed knowledge about their origin, composition, and temporal development is to date still lacking.

Present-day oceanographic circulation in the GoC is dominated by the exchange of water masses between the Atlantic Ocean and the Mediterranean Sea (Ochoa and Bray, 1991). The relatively cold Atlantic Inflow Water flows eastward along the Iberian margin partly entering the Mediterranean Sea. It is composed of North Atlantic Surficial Water and North Atlantic Central Water (NACW). The upper-thermocline NACW deepens from about 300 m water depth close to the Strait of Gibraltar to about 600 m in the outer and southern parts of the gulf (Ochoa and Bray, 1991; Mauritzen et al., 2001). Below this level occurs Mediterranean Outflow Water (MOW). Flowing westwards through the Strait of Gibraltar, the MOW prevails in the northern gulf where it flows between ~500 and 1 400 m water depth above the North Atlantic Deep Water (NADW) (Ambar et al., 1999; Baringer and Price, 1999) and acts as a strong contour current (García et al., 2009). It is characterised by a permanent salinity maximum of ~36-37 and temperatures of 10.5 to 12°C (Fusco et al., 2008). For the southern GoC along the Moroccan Atlantic margin information about its hydrography is basically lacking (Machín et al., 2006). However, Pelegrí et al. (2005) suggests the presence of MOW at 800 m. This assumption is supported by the presence of an anticyclone or meddy close to the Moroccan shelf which implies at least some temporary southward transport of MOW along the Moroccan margin (Carton et al., 2002).

Today, the GoC constitutes an oligotrophic system with diminished primary production in the surface waters (Behrenfeld et al., 2005). Cold and productive upwelling is restricted to a

narrow band along the Portuguese coast (Garcia-Lafuente and Ruiz, 2007), and to the NW African margin south of 31°N (Cape Ghir) (Mittelstaedt, 1991; Pelegrí et al., 2005). Due to a prevailing anticyclonic circulation (Pelegrí et al., 2005), the basin of the GoC separates the Iberian upwelling from the upwelling off NW Africa (Garcia-Lafuente and Ruiz, 2007).

3. Material and methods

3.1 Core locations

During three expeditions between 2003 and 2006, a set of ten coral-bearing sediment cores was collected from various sites in the GoC (Table 1). The coring sites comprise two mud volcanoes (Hespérides and Faro) along the Spanish margin and coral mounds along the Moroccan margin which are situated on top of the prominent Renard Ridge and its easternmost extension, the Pen Duick Escarpment. Finally, the southernmost core was collected north of Meknes mud volcano (Fig. 1).

The sediment cores have a length between 2.2 m and 8.6 m and are made up of abundant cold-water coral fragments embedded in a hemipelagic sediment matrix (Table 1). The sediment cores collected from mud volcanoes along the Spanish margin only contain cold-water corals in their upper parts, whereas the cores retrieved from coral mounds along the Moroccan margin are characterised by the occurrence of coral fragments throughout the sedimentary record.

To reconstruct oceanographic and environmental changes in the GoC during the last glacial-interglacial cycle and to compare this with the temporal distribution pattern of cold-water corals, sediment core GeoB 9064 (35°24.91'N, 06°50.72'W, 702 m water depth) was selected for a multiproxy study (Fig. 1). Core GeoB 9064 was collected along the Moroccan

133 margin (RV *Sonne* cruise SO175) and has a total length of 5.4 m. Samples for the various
134 analyses were taken in 5-cm-intervals.
135
136 **3.2 U/Th age determination on coral fragments**
137 Forty fragments of the reef-forming scleractinian coral species *Madrepora oculata* and
138 *Lophelia pertusa* were sampled at different core depths from the sediment cores listed in
139 Table 1. Uranium-series measurements were performed using multi-collector ICP and
140 thermo-ionization mass spectrometry at IFM-GEOMAR (Kiel, Germany; Fietzke et al., 2005)
141 and at LSCE (Gif-sur-Yvette, France; Frank et al., 2004; Douville et al., 2010). Prior to
142 analyses, samples were carefully cleaned to remove contaminants from the fossil skeleton
143 surfaces according to procedures described by Fietzke et al. (2005) and Frank et al. (2004).
144 Isotope concentrations and ratios as well as the absolute dates on the cold-water corals are
145 provided in Table 2. Whole procedure blank values of this sample set were measured to be
146 around 2 pg for thorium (Th) and between 4 and 8 pg for uranium (U). Both values are
147 negligible compared to U- and Th-concentrations of the studied corals. The reproducibility
148 of mass spectrometric measurements was tested using international U standard materials
149 such as HU1 and NBL112, which provided identical values as the ones published by Fietzke
150 et al. (2005) and Frank et al. (2004).
151
152 **3.3 Analyses on core GeoB 9064**
153 **3.3.1 AMS radiocarbon dating**
154 Accelerator mass spectrometry (AMS) dating was performed at the Leibniz Laboratory for
155 Age Determinations and Isotope Research (University of Kiel, Germany; Nadeau et al.,
156 1997) and at the Poznań Radiocarbon Laboratory (Poznań, Poland). AMS ^{14}C dates were
157 determined on ~8 mg calcium carbonate of mixed planktonic foraminifera. All ages were
158 corrected for ^{13}C and a mean ocean reservoir age of 400 years (Bard, 1988). AMS ^{14}C ages

were converted to calendar years using the CALPAL 2007 Hulu software (Joeris and Weninger, 1998) and are reported as calendar years before present (ka; Table 3).

3.3.2 Stable oxygen isotopes

The stable oxygen isotope ($\delta^{18}O$) composition of the planktonic foraminifera *Neogloboquadrina pachyderma* (dex.) was measured with a Finnigan MAT 251 mass spectrometer (Isotope Laboratory of the Department of Geosciences, University of Bremen, Germany). The isotopic composition was measured on the CO_2 gas evolved by treatment with phosphoric acid at a constant temperature of 75°C. A working standard (Burgbrohl CO_2 gas) was applied, which has been calibrated against PDB by using the NBS18, 19 and 20 standards. Consequently, all $\delta^{18}O$ data presented here are given relative to the PDB standard. Analytical standard deviation was about ±0.07‰.

3.3.3 Grain-size analysis and end-member modelling

Grain sizes were measured on bulk and terrigenous material using a Malvern Instruments Mastersizer 2000 (Hydraulic Research Laboratory, Borgerhout, Belgium), which determines particle grain sizes between 0.26 µm and 2 046 µm grouped into 66 size classes. The terrigenous sediment fraction was obtained by treating bulk sediment with H_2O_2 (30% at 85°C) and HCl (10% at 100°C) to remove organic carbon and calcium carbonate, respectively. The sediments contained negligible amounts of biogenic opal, and microscopic analyses revealed that the applied method successfully removed all biogenic constituents. Finally, the samples were suspended in demineralised water by stirring and ultrasonic dispersion before analysis.

The terrigenous fraction of deep-sea sediments in the ocean is considered a mixture of ice-rafted, aeolian, and fluvial transported sediments. End-member modelling allows the

distinction between possible lithic subpopulations of the grain-size spectrum (Weltje, 1997) that can be assigned to different sediment transport mechanisms (e.g., Stuut et al., 2002; Holz et al., 2007). To estimate the minimum number of end-members (EM) required for a satisfactory approximation of the data, the coefficients of determination were calculated. These coefficients represent the proportion of the variance of each grain-size class that can be reproduced by the approximated data. This proportion is equal to the squared correlation coefficient (r^2) of input variables and their approximated values (Weltje, 1997; Prins and Weltje, 1999). As the terrigenous sediment fraction from the southern GoC is relatively fine-grained (<170 µm), the number of input variables for the end-member model of core GeoB 9064 was reduced from 66 to 47 classes in the range of 0.29-170 µm.

3.3.4. Planktonic foraminiferal assemblage

The analysis for planktonic foraminiferal relative abundance counts is based on the >150 µm fraction. For each sample a minimum of ~200 specimens were identified following the taxonomy of planktonic foraminifera proposed by Hemleben et al. (1989). For *Neogloboquadrina pachyderma* the relative abundances of right (dex.) and left (sin.) coiling individuals were determined, and the two forms were treated as individual species. The data are represented as percentages of total planktonic foraminiferal number.

4. Results

4.1. U-series dating

All selected coral fragments indicated minor to moderate physico-chemical alteration or dissolution which may disturb U-series ages. Initial $\delta^{234}U_0$ values are variable and range between 125.9±2.7‰ to 187.1±2.6‰ (Table 2, Fig. 2). Measured ^{232}Th concentrations are small (<10 ng g^{-1}) for 75% of all samples (Fig. 2) but clearly specimens of *Madrepora oculata* reveal more residual Th then *Lophelia pertusa* (Table 2). This is a consequence of the

211 cleaning procedure as the thinner polyps and more fragile skeleton of *M. oculata* is by far
212 more difficult to clean. However, Th contamination is negligible since in general the
213 $^{230}Th/^{232}Th$ activity ratios are >1 000.
214
215 Calculated U-series ages from all investigated coral sites in the GoC range from 9.2 ka to
216 more than 400 ka (Fig. 3). Two samples from core GeoB 12101 could not be dated due to
217 above equilibrium radioactive isotopic composition indicating U-series open system
218 behaviour. More than 90% of all obtained ages correspond to glacial periods (Marine
219 Isotope Stage (MIS) 2 back to MIS12), and 70% of these glacial coral ages cluster within the
220 last glacial (MIS2-4) (Fig. 3). With regard to the initial $\delta^{234}U_0$, it is evident that the scatter
221 increases largely beyond a coral age of 150 ka which is clearly indicative of increasing U-
222 series system opening (Thompson et al., 2003; Scholz et al., 2004; Frank et al., 2006;
223 Robinson et al., 2006). Consequently, those ages are less precise than the measured
224 uncertainty would suggest which has to be taken in consideration for our data
225 interpretation. Corals ages between 14 and 60 ka yield a mean initial $\delta^{234}U_0$ of 143.2±2.3‰
226 (n=22, 2σ standard deviation), which is slightly lower than measured in modern corals and
227 seawater (146.6-149.6‰; Delanghe et al., 2002; Robinson et al., 2004). Thus either corals
228 suffer from minor U-series system opening, and thus, preferential loss of ^{234}U, or the glacial
229 mean value of seawater was slightly lower than compared to today as suggested by Esat et
230 al. (1999). Overall we consider that within a range of 149±10‰ calculated ages are
231 representing the chronological ages of the corals within the uncertainty of measurement
232 (see also Stirling et al., 1998; Robinson et al., 2004; Esat and Yokoyama, 2006). However,
233 we are aware that a more detailed analysis of the U-series data and uncertainties
234 considering potential seawater U-isotopic variations, diagenetic alteration and U-series
235 system opening is needed to improve in particular the quality of coral ages beyond 150 ka.
236

4.2. Age model core GeoB 9064

The age model of core GeoB 9064 for the last ~40 kyr is based on six AMS ^{14}C age control points and linear interpolation between these dates (Table 3, Fig. 4). The age model is supported by the correlation of the $\delta^{18}O$ measurements of the record (showing heavy $\delta^{18}O$ values of 1.5-2.5‰ for the last glacial and light values of <1.0‰ for the Holocene; Fig. 4) with the $\delta^{18}O$ record of the GRIP ice core (GRIP Members, 1993). The estimated average sedimentation rate is ~16 cm ka^{-1} (Table 3). Highest sedimentation rates of 18-24 cm ka^{-1} occur during MIS3 and the last deglaciation. Lowest sedimentation rates of 8-9 cm ka^{-1} are obtained for MIS2 and the Holocene (Fig. 4).

4.3. Grain size distribution and source

The median grain size of the terrigenous (bulk) fraction of sediment core GeoB 9064 varies between 5.71 µm (5.93 µm) and 12.03 µm (17.88 µm). The last glacial period and the Younger Dryas (YD) cold event are characterised by relatively coarse sediment deposition. In contrast, during the Holocene a distinct and continuous decrease of grain sizes is clearly visible (6-9 µm) (Fig. 4). A three-end-member model was created (with r^2=0.77) to describe the grain size data set of core GeoB 9064. The grain size distributions of the three end members are all unimodal, well-sorted and have relatively fine modal grain sizes with 25 µm for EM1, 16 µm for EM2, and 5 µm for EM3. Several sedimentological studies confirmed that aeolian sediments deposited in the deep-sea close to the continent are coarser grained than hemipelagic sediments with terrigenous sediments with mean grain sizes >6 µm being generally attributed to aeolian transport, and sediments <6 µm to hemipelagic transport (Ratmeyer et al., 1999; Prins et al., 2000). In addition, the mean modal sizes of present-day aeolian dust, collected along a transect of the NW African coast (33°N to 12°S) vary between 8 µm and 42 µm (Stuut et al., 2005). Hence, for core GeoB 9064, the two coarsest end members of the three-end-member model are considered to be of aeolian origin with EM1

interpreted as 'coarse' aeolian dust and EM2 as 'fine' aeolian dust. In contrast, EM3 is interpreted to result predominantly from fluvial input (Koopmann, 1981; Holz et al., 2007). During the last glacial, the aeolian content varies considerably between 30% and 60% and shows in particular during MIS3 rapid fluctuations. Close to the end of the last glacial (~17 ka), the aeolian content decreases before it increases again up to 60% during the YD. With the end of the YD (~11.5 ka), the proportion of the aeolian content on the total terrigenous fraction decreases continuously down to 25% (Fig. 4).

The EM1/EM2-ratio is considered as a measure for the relative wind intensity (Stuut et al., 2002). For core GeoB 9064, relatively high wind strength is indicated for the last glacial showing millennial-scale fluctuations. At ~22 ka, the wind conditions changed dramatically. Within a time period of 1.5 kyr, wind intensity decreased remarkably by 50% and stayed low during the entire Holocene (Fig. 4). This is deduced from a reduction of the content of 'coarse' aeolian dust (EM1) to almost zero, whereas the 'fine' aeolian dust (EM2) slightly increased towards the present.

4.4. Planktonic foraminiferal assemblage and abundance

The most abundant species in core GeoB 9064 is *Neogloboquadrina pachyderma* dex. (27.1%), followed by *Globigerinita glutinata* (21.1%), *Globigerina bulloides* (15.8%), and *Globorotalia inflata* (12.2%). Together with *Globigerinoides ruber* (5.2%), *Globorotalia scitula* (4.5%), and *N. pachyderma* sin. (4.5%), these species account on average for >90% of the total planktonic foraminifera.

Maximum relative abundances of *N. pachyderma* dex. is recorded during the last glacial, contributing up to 60% of the total planktonic foraminifera fauna. At the end of the last glacial (15.5-14.5 ka), its relative abundances decreased remarkably down to 10%, followed by an increase up to 40% during the YD. At the end of the YD (~11.5 ka), relative abundances of *N.*

290 *pachyderma* dex. significantly decreased down to <5% (Fig. 5). A similar trend is indicated for
291 *N. pachyderma* sin., although it shows comparably lower abundances below 18%. Another
292 abundant species during the last glacial was *G. glutinata* with relative abundances of 10-40%.
293 During the course of the Holocene, its contribution was rather low with minimum rates of
294 <10% except for the period between 10 and 8.5 ka, with relative abundances of up to 28%. An
295 opposite trend to the above mentioned species is observed for *G. bulloides*. Relatively low
296 abundance occurred during the last glacial (<20%), whereas during the Holocene, its relative
297 contribution to the total fauna increased to >20%. In particular between 8.5 and 2 ka, *G.*
298 *bulloides* was the most common species within the planktonic foraminiferal fauna with
299 relative abundance of 30-48%. Between 40 and 18 ka, abundances of *G. inflata* were below
300 20%, and increased up to 38% until the onset of the YD. During the Holocene, its abundances
301 varied between 8% and 20%. One distinct minimum (<10%) of *G. inflata* abundance is
302 indicated between 10 and 8.5 ka that mirrors the concomitant maxima of *G. glutinata*.
303 Contributions of *G. scitula* to the total fauna was rather moderate for most of the last glacial,
304 and decreased remarkably around 18 ka to <5%, and remained low thereafter (Fig. 5). During
305 the last glacial and until the end of the YD (~11.5 ka), *G. ruber* shows a low abundance of 0-
306 10% that increased to 10-25% during the Holocene. *Globigerinoides sacculifer* was even
307 absent during the last glacial. This species is exclusively found during the Holocene with
308 relative abundances of up to 7.5% (Fig. 5).
309

310 **5. Discussion**

311 **5.1. Glacial coral growth phases in the Gulf of Cádiz**

312 During the past years, much effort has been invested into dating cold-water corals from
313 various sites along the NE Atlantic margin. The most comprehensive data set of coral ages
314 exists for the Irish margin and reveals that coral growth in this area is restricted to the
315 Holocene and prior interglacial periods (Frank et al., 2005; Rüggeberg et al., 2007; de Haas

et al., 2009; Frank et al., 2009). In contrast, for coral sites south of 50°N the data set of coral ages is rather scattered. However, the available dates suggest that the major phase of coral growth along the French, Iberian and Moroccan margins coincide with the last glacial period (Taviani et al., 1991; Schröder-Ritzrau et al., 2005; Wienberg et al., 2009).

For the GoC, it was shown that the reef-forming coral species *Lophelia pertusa* and *Madrepora oculata* have been restricted to a period between 12 and 45 ka (Wienberg et al., 2009). This preliminary result is confirmed by our data. In addition, the U/Th dates presented here show that major phases of coral growth in the GoC are not solely restricted to the last glacial but also to prior glacial periods (back to MIS12), whereas during interglacials coral growth seems to be reduced or even absent (Fig. 2).

Most conspicuous is that the widespread decline of the coral ecosystems in the GoC during the YD cold reversal (12.9–11.5 ka) corresponds to the re-start of coral mound formation on Rockall Bank and the re-establishment of coral mound growth along the slopes of the Porcupine Seabight at around 11 ka (Frank et al., 2009). Regarding this pattern, we suggest that at the transition of the last glacial-interglacial, a latitudinal shift of areas with optimum cold-water coral growth conditions towards the northern NE Atlantic occurred that was most probably related to dramatic changes of the oceanographic and environmental conditions caused by climate change. Moreover, this northward shift happened rapidly over just a few hundreds of years and over a distance of 2 000-2 500 km (GoC to Irish margin).

Unfortunately, we still lack detailed understanding of the reproductive ecology and larval dispersal mode of scleractinian cold-water corals. Histological studies show that the cosmopolitan species *L. pertusa* exhibits an annual gametogenic cycle with spawning around January/February (Waller and Tyler, 2005). The widespread occurrence of *L. pertusa* and the rapid colonisation of man-made structures such as oil rigs (25 mm $year^{-1}$; Bell and

343 Smith, 1999), point to a dispersive planula larva being capable to remain in the water
344 column for several weeks.
345
346 **5.2. Driving factors for coral growth**
347 A combination of environmental and oceanographic conditions is required to promote a
348 sustained development of cold-water coral ecosystems. Cold-water corals require (1) hard
349 substrate to settle on, (2) protection against burial to grow, and (3) sufficient food supply.
350 Therefore, they predominate in areas where strong currents prevail that reduce deposition
351 of fine-grained sediments and supply large quantities of food (Roberts et al., 2006). Today,
352 thriving coral ecosystems occur in high concentrations in areas that are characterised by
353 enhanced primary production in the surface waters of eutrophic systems, allowing a
354 considerable part of the new production to be transported to the seafloor. In addition, tidal
355 currents and internal waves have been identified (1) to enhance concentrations of organic
356 matter at the shelf edge and (2) to transport fresh food particles to and through the cold-
357 water coral reefs (Frederiksen et al., 1992; White et al., 2005; White et al., 2007). Recently,
358 Dullo et al. (2008) indicated for the Celtic and Nordic margins that living cold-water corals
359 occur within the density envelope of sigma-theta (σ_Θ)=27.35-27.65 kg m^{-3} emphasising the
360 importance of physical boundary conditions. Finally, the world's most common cold-water
361 coral species *Lophelia pertusa* tends to be associated with oceanic water masses with a
362 temperature of 4-12°C (Roberts et al., 2006), and even up to 14°C in the Mediterranean Sea
363 (Taviani et al., 2005; Freiwald et al., 2009), salinities between 31.7 and 38.78 (Freiwald et
364 al., 2004; Davies et al., 2008), and oxygen concentrations of 4.3-7.2 ml l^{-1} (for the NE
365 Atlantic; Davies et al., 2008).
366
367 For the GoC, all these requirements must have been fulfilled during glacial periods as cold-
368 water corals were widespread during these times. During interglacial periods, these optimal
369 environmental and oceanographic conditions must have been changed dramatically

370 resulting in a widespread (gulf-wide) demise of the formerly thriving corals. As our obtained
371 coral ages mainly cluster within the last glacial (~70%), the environmental and
372 oceanographic changes of the GoC, focussing on the last glacial-interglacial cycle, are
373 discussed in detail to identify the main forcing factors for coral growth in the GoC.
374

375 **5.2.1 Effects of increased palaeo-productivity on cold-water coral growth**

376 Strong vertical fluxes of labile organic matter, as often found in eutrophic regions, result in
377 rich benthic fauna (e.g., De Stigter et al., 1998; Schmiedl et al., 2000; Fontanier et al., 2002).
378 In the NE Atlantic, seasonal algae blooms that sink rapidly to the deep-sea floor can even
379 have a positive effect on the reproductive biology of benthic invertebrates (Billett et al.,
380 1983; Thiel et al., 1989; Tyler et al., 1992), a relationship which is also hypothesised for
381 *Lophelia pertusa* and *Madrepora oculata* thriving along the Irish margin (Waller and Tyler,
382 2005). Thus, enhanced productivity is a pre-requisite for a sustained development of
383 healthy cold-water coral ecosystems. Indeed, regions with enhanced primary production as
384 deduced from satellite-based observations of the chlorophyll content in surface waters
385 (Behrenfeld et al., 2005) seem to mirror the recent distribution of thriving coral sites in the
386 NE Atlantic.
387

388 Certain species of planktonic foraminifera strongly depend on primary productivity in the
389 modern ocean (Hemleben et al., 1989), and hence downcore variations of the abundance of
390 planktonic foraminiferal species within sedimentary records can be applied to assess
391 palaeo-productivity conditions (e.g., Ivanova et al., 2003). In this context, the
392 environmental constraints of the most abundant foraminiferal species identified for the
393 GoC are reviewed in detail.
394

395 *Globigerina bulloides* mainly thrives in the surface mixed layer above the thermocline and
396 prefers relatively cold and nutrient-rich waters (e.g., Ganssen and Kroon, 2000; Chapman,

2010). Moreover, this species preferably occurs in areas along the Iberian and NW African margins that are characterised by pronounced seasonal upwelling, and thus, by high phytoplankton density and prey abundance (Salgueiro et al., 2008; Wilke et al., 2009). The opportunistic and cosmopolitan species *Globigerinita glutinata* is also strongly associated with the increase in productivity during spring bloom events in the North Atlantic (Chapman, 2010). However, the distribution of this species is found to be even more significantly associated with productivity than that of *G. bulloides*, which can be explained by its diet that preferentially consists of diatoms (Bé and Tolderlund, 1971; Hemleben et al., 1989; Schiebel et al., 2001). The sub-polar species *Neogloboquadrina pachyderma* dex. prefers colder waters than *G. bulloides* (Bé and Tolderlund, 1971). Off the northern Iberian margin, high percentages of this species have been related to increased productivity generated by high river runoff (Salgueiro et al., 2008). In the GoC, *G. glutinata* and *N. pachyderma* dex. clearly dominate the foraminiferal assemblage during the last glacial with relative abundances of 55 to 75% (Fig. 5), thus pointing to rather nutrient-rich and cold conditions compared to the following Holocene when both species account for only ~10%. However, although *G. bulloides* is regarded as an indicator for nutrient enriched conditions it shows an opposite trend compared to the other two species.

Globorotalia inflata is considered a non-upwelling species and high relative abundances of this species in the North Atlantic coincide with oligotrophic waters (Pflaumann et al., 2003; Salgueiro et al., 2008). The two surface-dwelling species *Globigerinoides ruber* and *Globigerinoides sacculifer* show a preference towards oligotrophic conditions as well (e.g., Ivanova et al., 2003; Mohtadi et al., 2007). These species prefer warm and well stratified surface waters (Duplessy et al., 1981; Stoll et al., 2007; Chapman, 2010). For the NE Atlantic, a significant increase in the relative abundances of *G. sacculifer* is observed when surface stratification is at a maximum and high sea surface temperatures prevail (Chapman, 2010). The significant increase of *G. ruber* and *G. sacculifer* after the YD cold event as found in

424 our record (Fig. 5) thus indicates such warm and well stratified conditions in the GoC during
425 the Holocene.
426
427 Taking all these findings for the NE Atlantic into account, *G. sacculifer*, *G. ruber* and *G.*
428 *inflata* are inferred to represent a low-productivity assemblage, whereas *G. glutinata*,
429 *G. bulloides* and *N. pachyderma* dex. are grouped as indicators for enhanced productivity.
430 Similar to the approach of Stoll et al. (2007), we calculated the ratio of both assemblages
431 and interpreted this ratio as an indicator of productivity (Fig. 4f), regardless of their affinity
432 to upwelling processes. This ratio clearly shows that during the last glacial palaeo-
433 productivity was overall enhanced in the GoC, which is in particular expressed by high
434 relative abundances of *G. glutinata* (Fig. 5). Following the end of the last glacial, this ratio
435 significantly changed towards more oligotrophic conditions (Fig. 4).
436
437 **5.2.2 Implications of frontal upwelling on glacial productivity in the GoC**
438 This pattern of eutrophic conditions during the last glacial and oligotrophic conditions
439 during the Holocene found for the GoC might be explained by a shift of the Azores Front
440 (Rogerson et al., 2004). The Azores Front marks a zone of strong hydrographic transition
441 associated with enhanced biological production caused by locally intense upwelling (Alves
442 and DeVerdière, 1999). Today, the easternmost extension of the Azores Front is situated at
443 30°N off the Moroccan margin (Gould, 1985; Schiebel et al., 2002), and hence, does not
444 penetrate into the GoC that extends from 37°N to 33°N (Fig. 1). But there is evidence that
445 the Azores Front shifted northward and thus penetrated eastward into the GoC prior to 16
446 ka and during the YD (Rogerson et al., 2004). Rogerson et al. (2004) indicated this glacial
447 shift of the Azores Front towards the GoC by high abundances of the planktonic foraminifer
448 *Globorotalia scitula* in their records. This deep-dwelling species (100-700 m water depth)
449 (Schiebel et al., 2002) is used as an indicator for cool surface waters and enhanced vertical
450 mixing at temperate latitudes (e.g., Thunell and Reynolds, 1984; Perez-Folgado et al., 2003).

Today *G. scitula* is found in high numbers in the Azores Front where upwelling causes high productivity (Schiebel et al., 2002), but it is almost absent in the GoC (Rogerson et al., 2004). The record of core GeoB 9064 shows that *G. scitula* is common prior to the Last Glacial Maximum (LGM), but is rare throughout the Holocene (Fig. 5) pointing to enhanced productivity during the last glacial caused by frontal upwelling.

5.2.3 Fertilisation effect of aeolian dust

Besides the effect of locally intensified upwelling that likely occurred in the GoC during the last glacial also the high input of aeolian dust might have significantly enhanced glacial productivity in the area. Grain size data from various sediment cores in the GoC, including our data (Fig. 4), show that during the last glacial mean grain sizes were rather coarse compared to the following Holocene (e.g., Rogerson et al., 2005; Voelker et al., 2006). Up to now, these grain size variations have been primarily attributed to changes in the strength of the prevailing bottom currents implying that bottom current strength was enhanced during the last glacial probably caused by a shift and intensification of the MOW's flow pathway (Schönfeld and Zahn, 2000; Rogerson et al., 2005; Voelker et al., 2006). Another common finding for the GoC is a rather low Holocene sedimentation rate (e.g., Rogerson et al., 2005; Voelker et al., 2006). Rogerson et al. (2005) estimated a Holocene accumulation rate that is only one fifth of that of the last glacial, and thus is in agreement with our estimated rates (Fig. 4). They assumed that this tremendous change in sedimentation rate was caused by a higher sediment supply prior to the last deglaciation but without indicating the major source of sediments supplied to the GoC.

However, this study shows that the variations in grain size and sedimentation rate as found for the GoC are rather the result of changes in the source of the terrigenous sediments and the amount of sediment input. Our grain size data clearly reveal that during the last glacial the deposition of aeolian transported sediments prevailed in the GoC (Fig. 4). During this

time rather arid and cold conditions prevailed over the NW African continent (Gasse, 2000), and the intensity of the northern trade winds, which transport the aeolian dust, was enhanced especially from about 36°N to 24°N (Sarnthein et al., 1981; Hooghiemstra et al., 1987; Moreno et al., 2002). This is supported by our record showing that wind strength off Morocco (35°N) was significantly enhanced during the last glacial (Fig. 4). With the end of the YD, the proportion of the aeolian content on the total terrigenous fraction decreased continuously from 60 to 25% (Fig. 4), corresponding to the African humid period, which is known to be characterised by a relatively humid and green Sahara with significantly lower amounts of aeolian dust being produced (e.g., deMenocal et al., 2000; Gasse, 2000). The African humid period terminated at 5.5 ka and the area of the Saharan desert returned to a state of hyperarid conditions (deMenocal et al., 2000). However, wind strength remained relatively low compared to the strong glacial trade winds (Hooghiemstra et al., 1987) and dust fluxes have been estimated to be today 2-4 times lower compared to the LGM (Grousset et al., 1998). Also our data show no significant increase of the input of aeolian dust in the GoC after 5.5 ka until today (Fig. 4).

The large input of aeolian dust during the last glacial coincides with a prosperous cold-water coral community in the GoC (Fig. 4). The link between dust input and coral prosperity was probably established by a simple fertilisation effect. During periods of enhanced Saharan dust input over the NE Atlantic, the supply of iron and manganese to the surface ocean is enhanced as well (de Jong et al., 2007) which promotes primary production in the surface waters (e.g., Boyd et al., 2000), and as a consequence, also might increase food availability for the bathyal cold-water corals.

5.2.4 Limitation of water temperatures on the prosperity of cold-water corals

The planktonic foraminiferal abundance data of core GeoB 9064 is consistent with the thermal history of the LGM and deglaciation. The general warming of the North Atlantic at

505 the transition from the last glacial to the Holocene is reflected by a considerable increase in
506 the abundance of *G. ruber* and *G. sacculifer* and a concurrent decrease in abundance of *N.*
507 *pachyderma* dex., which is even more pronounced after the YD cold reversal (Fig. 5). This
508 pattern is in agreement with other foraminiferal fauna records from the GoC (Sierro et al.,
509 1999; Rogerson et al., 2004). The change from rather cool towards warm surface waters
510 after the end of the YD was most likely accompanied by a change in subsurface
511 temperatures in intermediate water depths, thus having an impact on the bathyal cold-
512 water corals. Regarding the average temperatures of the intermediate water masses
513 prevailing in the GoC (NACW: ~12°C, Ait-Ameur and Goyet, 2006; MOW: 10.5-12°C, Fusco et
514 al., 2008), it becomes obvious that at least today water temperatures are at the very upper
515 tolerance for reef-forming scleractinian cold-water corals such as *Lophelia pertusa* (12°C;
516 Roberts et al., 2006). Moreover, dendrophylliid coral species that prefer rather warm
517 conditions compared to *L. pertusa* seem to have been more common during the late
518 Holocene (Wienberg et al., 2009).
519
520 **6. Conclusion**
521 This study clearly shows that the occurrence of cold-water corals in the GoC is dominant
522 within the last glacial and prior glacial periods and that hardly any cold-water corals exist in
523 this region during interglacials. Moreover, it could be identified that at the end of the YD
524 cold event a shift from eutrophic to oligotrophic and warm conditions have been
525 responsible for the demise of the formerly thriving coral ecosystems. The enhanced
526 productivity conditions during the last glacial have been most probably caused by (1) an
527 enhanced input of aeolian dust and (2) a shift of the Azores Fronts towards the GoC causing
528 locally intense upwelling. Both factor supported enhanced primary productivity in the GoC,
529 and thus resulted in enhanced food availability for the corals. By comparing our data set for
530 the GoC with coral ages from the Norwegian and Irish margins that reveal a sustained
531 prosperity of coral ecosystems right after the YD, it appears that a northward shift of areas

with optimum cold-water coral growth conditions took place during the transition from the last glacial to the recent interglacial. The cold-water corals responded very rapidly to climate change over just a few hundreds of years, and it is most likely that in the course of global warming going along with dramatic changes in the environmental setting this northward trend will further continue.

Acknowledgements

The research leading to these results (U/Th and radiocarbon dates) has received funding from the European Community's Seventh Framework Programme (FP7/2007-2013) under the HERMIONE project, grant agreement n° 226354. In addition, this work is part of CARBONATE (palaeo-environmental reconstructions), an ESF EUROCORES integrated project as part of the EuroMARC project cluster funded by the DFG. K.M. Mertens is a Postdoctoral Researcher funded by the FWO. M. Marchant acknowledges the Dirección de Investigación and Departamento de Zoología at the University of Concepción (Chile) and the German Academic Exchange Service (DAAD). On-board assistance by ship and scientific team during cruises SO175 with RV Sonne (2003), 64PE229 with RV Pelagia (2004) and MSM01-3 with RV Maria S. Merian (2006) is acknowledged. O. Pfannkuche, J. Schönfeld and L. Maignien are kindly thanked for their great scientific support during cruise MSM01-3. We further acknowledge the support of the staff of the LSCE Gif-sur-Yvette (E. Douville, E. Sallé, C. Noury), the German Leibniz Laboratory for Age Determination and Isotope Research (University of Kiel, Germany), and the Poznan Radiocarbon Laboratory (Poznan, Poland) in U/Th and radiocarbon dating as well as the staff of the UGhent (M. Verreth, A. Raes, F. Mostaert) in sample preparation and grain size analysis. Finally, A. Eisenhauer, M. Mohtadi and two anonymous reviewers are kindly thanked for helpful discussions and comments.

References

Ait-Ameur, N., Goyet, C., 2006. Distribution and transport of natural and anthropogenic CO_2 in the Gulf of Cádiz. Deep-Sea Res. II 53, 1329–1343.

Alves, M., DeVerdière, A.C., 1999. Instability dynamics of a subtropical jet and applications to the Azores Front current system: Eddydriven mean flow. J. Physic. Oceanogr. 29, 837-864.

Ambar, I., Armi, L., Bower, A., Ferreira, T., 1999. Some aspects of time variability of the Mediterranean outflow. Deep-Sea Res. 26A, 1109-1136.

Bard, E., 1988. Correction of accelerator mass spectrometry ^{14}C ages measured in planktonic foraminifera: Paleoceanographic implications. Paleoceanography 3, 635-645.

Baringer, M.O., Price, J.F., 1999. A review of the physical oceanography of the Mediterranean outflow. Mar. Geol. 155, 63-82.

Bé, A.W.H., Tolderlund, D.S., 1971. Distribution and ecology of living planktonic foraminifera in surface waters of the Atlantic and Indian Oceans. In: Funel, B.M., Riedel, W.R. (Eds.), The Micropaleontology of Oceans. Cambridge University Press, pp. 105-149.

Behrenfeld, M.J., Boss, E., Siegel, D.A., Shea, D.M., 2005. Carbon-based ocean productivity and phytoplankton physiology from space. Glob. Biogeochem. Cycl. 19, GB1006, doi:1010.1029/2004GB002299.

Bell, N., Smith, J.E., 1999. Coral growing on North Sea oil rigs. Nature 402, 601.

Billett, D.S.M., Lampitt, R.S., Rice, A.L., Mantoura, R.F.C., 1983. Seasonal sedimentation of phytoplankton to the deep-sea benthos. Nature Geosci. 302, 520-522.

Boyd, P.W., Watson, A.J., Law, C.S., Abraham, E.R., Trull, T., Murdoch, R., Bakker, D.C.E., Bowie, A.R., Buesseler, K.O., Chang, H., Charette, M., Croot, P., Downing, K., Frew, R., Gall, M., Hadfield, M., Hall, J., Harvey, M., Jameson, G., LaRoche, J., Liddicoat, M., Ling, R., Maldonado, M.T., McKay, R., Nodder, S., Pickmere, S., Pridmore, R., Rintoul, S., Safi, K., Sutton, P., Strzepek, R., Tanneberger, K., Turner, S., Waite, A., Zeldis, J., 2000.

577 *A mesoscale phytoplankton bloom in the polar Southern Ocean waters stimulated by iron fertilization. Nature*
578 *407, 695-702.*
579 *Carton, X., Chérubin, L., Paillet, J., Morel, Y., Serpette, A., Le Cann, B., 2002. Meddy coupling with a deep cyclone*
580 *in the Gulf of Cádiz. J. Mar. Syst. 32, 13-42.*
581 *Chapman, M.R., 2010. Seasonal production pattern of planktonic foraminifera in the NE Atlantic Ocean:*
582 *Implications for paleotemperature and hydrographic reconstructions. Paleoceanography 25, PA1101,*
583 *doi:10.1029/2008PA001708.*
584 *Colman, J.G., Gordon, D.M., Lane, A.P., Forde, M.J., Fitzpatrick, J., 2005. Carbonate mounds off Mauritania,*
585 *Northwest Africa: status of deep-water corals and implications for management of fishing and oil exploration*
586 *activities. In: Freiwald, A., Roberts, J.M. (Eds.), Cold-water Corals and Ecosystems. Springer, Heidelberg, pp.*
587 *417-441.*
588 *Davies, A.J., Wisshak, M., Orr, J.C., Roberts, J.M., 2008. Predicting suitable habitat for the cold-water coral*
589 *Lophelia pertusa (Scleractinia). Deep-Sea Res. I 55, 1048-1062.*
590 *de Haas, H., Mienis, F., Frank, N., Richter, T.O., Steinbacher, R., de Stigter, H., van der Land, C., van Weering,*
591 *T.C.E., 2009. Morphology and sedimentology of (clustered) cold-water coral mounds at the south Rockall*
592 *Trough margins, NE Atlantic Ocean. Facies 55, 1-26.*
593 *de Jong, J.T.M., Boyé, M., Gelado-Caballero, M.D., Timmermans, K.R., Veldhuis, M.J.W., Nolting, R.F., van den*
594 *Berg, C.M.G., de Baar, H.J.W., 2007. Inputs of iron, manganese and aluminium to surface waters of the*
595 *Northeast Atlantic Ocean and the European continental shelf. Mar. Chem. 107, 120-142.*
596 *De Stigter, H.C., Jorissen, F.J., Vand der Zwaan, G.J., 1998. Bathymetric distribution and microhabitat partitioning*
597 *of live (Rose Bengal stained) benthic foraminifera along a shelf to deep sea transect in the southern Adriatic*
598 *Sea. J. Foram. Res. 28, 40-65.*
599 *Delanghe, D., Bard, E., Hamelin, B., 2002. New TIMS constraints on the uranium-238 and uranium-234 in*
600 *seawaters from the main ocean basins and the Mediterranean Sea. Mar. Chem. 80, 79-93.*
601 *deMenocal, P., Ortiz, J., Guilderson, T., Adkins, J., Sarnthein, M., Baker, L., Yarusinsky, M., 2000. Abrupt onset*
602 *and termination of the African Humid Period:: rapid climate responses to gradual insolation forcing. Quat. Sci.*
603 *Rev. 19, 347-361.*
604 *Dorschel, B., Hebbeln, D., Rüggeberg, A., Dullo, W.-C., 2005. Growth and erosion of a cold-water coral covered*
605 *carbonate mound in the Northeast Atlantic during the Late Pleistocene and Holocene. Earth Planet. Sci. Lett.*
606 *233, 33-44.*
607 *Douville, E., Sallé, E., Frank, N., Eisele, M., Pons-Branchu, E., Ayrault, S., 2010. Rapid and accurate Th-U dating of*
608 *ancient carbonates using Inductively Coupled Plasma-Quadrupole Mass Spectrometry. Chem. Geol. 272, 1-11.*
609 *Duineveld, G.C.A., Lavleye, M.S.S., Berghuis, E.M., 2004. Particle flux and food supply to a seamount cold-water*
610 *coral community (Galicia Bank, NW Spain). Mar. Ecol. Prog. Ser. 277, 13-23.*
611 *Dullo, C., Flögel, S., Rüggeberg, A., 2008. Cold-water coral growth in relation to the hydrography of the Celtic and*
612 *Nordic European continental margin. Mar. Ecol. Prog. Ser. 371, 165-176.*
613 *Duplessy, J.C., Bé, A.W., Blanc, P.L., 1981. Oxygen and carbon isotopic composition and biogeographic*
614 *distribution of planktonic foraminifera in the Indian Ocean. Palaeogeogr. Palaeoclimat. Palaeoecol. 33, 9-46.*
615 *Eisele, M., Hebbeln, D., Wienberg, C., 2008. Growth history of a cold-water coral covered carbonate mound -*
616 *Galway Mound, Porcupine Seabight, NE-Atlantic. Mar. Geol. 253, 160-169.*
617 *Esat, T.M., McCulloch, M.T., Chappell, J., Pillans, B., Omura, A., 1999. Rapid fluctuations in sea level recorded at*
618 *Huon Peninsula during the penultimate deglaciation. Science 283, 197-201.*
619 *Esat, T.M., Yokoyama, Y., 2006. Variability in the uranium isotopic composition of the oceans over glacial-*
620 *interglacial timescales. Geochim. Cosmochim. Acta 70, 4140-4150.*
621 *Fietzke, J., Liebetrau, V., Eisenhauer, A., Dullo, W.-C., 2005. Determination of uranium isotope ratios by multi-*
622 *static MIC-ICP-MS: method and implementation for precise U- and Th-series isotopes. J. Anal. Atomic Spectrom.*
623 *20, 395-401.*
624 *Fontanier, C., Jorissen, F.J., Licari, L., Alexandre, A., Anshutz, P., Carbonel, P., 2002. Live benthic foraminiferal*
625 *faunas from the Bay of Biscay: faunal density, composition, and microhabitats. Deep-Sea Res. I 49, 751-785.*
626 *Fosså, J.H., Lindberg, B., Christensen, O., Lundälv, T., Svellingen, I., Mortensen, P.B., Alsvag, J., 2005. Mapping of*
627 *Lophelia reefs in Norway: experiences and survey methods. In: Freiwald, A., Roberts, J.M. (Eds.), Cold-water*
628 *Corals and Ecosystems. Springer, Heidelberg, pp. 359-391.*
629 *Foubert, A., Depreiter, D., Beck, T., Maignien, L., Pannemans, B., Frank, N., Blamart, D., Henriet, J.-P., 2008.*
630 *Carbonate mounds in a mud volcano province off north-west Morocco: key to processes and controls. Mar.*
631 *Geol. 248, 74-96.*
632 *Frank, N., Paterne, M., Ayliffe, L., van Weering, T.C.E., Henriet, J.-P., Blamart, D., 2004. Eastern North Atlantic*
633 *deep-sea corals: tracing upper intermediate water $\Delta^{14}C$ during the Holocene. Earth Planet. Sci. Lett. 219, 297-*
634 *309.*
635 *Frank, N., Lutringer, A., Paterne, M., Blamart, D., Henriet, J.-P., van Rooij, D., van Weering, T.C.E., 2005. Deep-*
636 *water corals of the northeastern Atlantic margin: carbonate mound evolution and upper intermediate water*
637 *ventilation during the Holocene. In: Freiwald, A., Roberts, J.M. (Eds.), Cold-water Corals and Ecosystems.*
638 *Springer, Heidelberg, pp. 113-133.*

639 *Frank, N., Turpin, L., Cabioch, G., Blamart, D., Tressens-Fedou, M., Colin, C., Jean-Baptiste, P., 2006. Open system*
640 *U-series ages of corals from a subsiding reef in New Caledonia: Implications for sea level changes, and*
641 *subsidence rate. Earth Planet. Sci. Lett. 249, 274-289.*
642 *Frank, N., Ricard, E., Lutringer-Paque, A., van der Land, C., Colin, C., Blamart, D., Foubert, A., Van Rooij, D.,*
643 *Henriet, J.-P., de Haas, H., van Weering, T.C.E., 2009. The Holocene occurrence of cold-water corals in the NE*
644 *Atlantic: Implications for coral carbonate mound evolution. Mar. Geol. 266, 129-142.*
645 *Frederiksen, R., Jensen, A., Westerberg, H., 1992. The distribution of scleratinian coral Lophelia pertusa around*
646 *the Faroe Islands and the relation to intertidal mixing. Sarsia 77, 157-171.*
647 *Freiwald, A., Fosså, J.H., Grehan, A., Koslow, T., Roberts, J.M., 2004. Cold-water Coral Reefs. UNEP-WCMC,*
648 *Biodiversity Series 22, Cambridge, UK, p. 84.*
649 *Freiwald, A., Beuck, L., Rüggeberg, A., Taviani, M., Hebbeln, D., R/V Meteor Cruise M70-1 participants, 2009. The*
650 *white coral community in the central Mediterranean Sea revealed by ROV surveys. Oceanography 22, 58-74.*
651 *Fusco, G., Artale, V., Cotroneo, Y., Sannino, G., 2008. Thermohaline variability of Mediterranean Water in the*
652 *Gulf of Cádiz, 1948-1999. Deep-Sea Res. I 55, 1624-1638.*
653 *Ganssen, G., Kroon, D., 2000. The isotopic signature of planktonic foraminifera from the NE Atlantic surface*
654 *sediments: implications for the reconstruction of past oceanic conditions. J. Geol. Soc. London 157, 693-699.*
655 *Garcia-Lafuente, J., Ruiz, J., 2007. The Gulf of Cádiz pelagic ecosystem: A review. Prog. Oceanogr. 74, 228-251.*
656 *García, M., Hernández-Molina, F.J., Llave, E., Stow, D.A.V., León, R., Fernández-Puga, M.C., Diaz del Río, V.,*
657 *Somoza, L., 2009. Contourite erosive features caused by the Mediterranean Outflow Water in the Gulf of Cádiz:*
658 *Quaternary tectonics and oceanographic implications. Mar. Geol. 257, 24-40.*
659 *Gasse, F., 2000. Hydrological changes in the African tropics since the Last Glacial Maximum. Quat. Sci. Rev. 19,*
660 *189-211.*
661 *Gould, W.J., 1985. Physical oceanography of the Azores Front. Prog. Oceanogr. 14, 167-190.*
662 *GRIP Members, 1993. Climate instability during the last interglacial period recorded in the the GRIP ice core.*
663 *Nature 364, 203-207.*
664 *Grousset, F.E., Parra, M., Bory, A., Martinez, P., Betrand, P., Shimmield, G., Ellam, R.M., 1998. Saharan wind*
665 *regimes traced by the Sr-Nd isotopic composition of subtropical Atlantic sediments: Last Glacial Maximum vs.*
666 *today. Quat. Sci. Rev. 17, 395-409.*
667 *Hebbeln, D., Wienberg, C., cruise participants, 2008. Report and preliminary results of RV Pelagia cruise*
668 *64PE284, Cold-water corals in the Gulf of Cádiz and on Coral Patch Seamount, Portimao - Portimao, 18.02.-*
669 *09.03.2008. University of Bremen, Reports of the Department of Geosciences (GeoB) No. 265, p. 90.*
670 *Hemleben, C., Spindler, M., Anderson, O.R., 1989. Modern Planktonic Foraminifera. Springer, New York, 363 pp.*
671 *Holz, C., Stuut, J.B., Meggers, H., Rüdiger, H., 2007. Variability in terrigenous sedimentation processes off*
672 *northwest Africa and its relation to climatic changes: inferences from grain-size distributions of a Holocene*
673 *marine sediment record. Sediment. Geol. 202, 499-508.*
674 *Hooghiemstra, H., Bechler, A., Beug, H.-J., 1987. Isopollen maps for 18,000 years BP of the Atlantic offshore of*
675 *Northwest Africa: Evidence for paleowind circulation. Paleoceanography 2, 561-582.*
676 *Imbrie, J., Hays, J.D., Martinson, D.G., McIntyre, A., Mix, A.C., Morley, J.J., Pisias, N.G., Prell, W.L., Shackleton,*
677 *N.J., 1989. The orbital theory of Pleistocene climate: support from a revised chronology of the marine $\delta^{18}O$*
678 *record. In: Berger, A. (Ed.), Milankovitch and Climate. NATO ASI Series, Dordrecht, pp. 269-305.*
679 *Ivanova, E., Schiebel, R., Singh, A.D., Schmiedl, G., Niebler, H.-S., Hemleben, C., 2003. Primary production in the*
680 *Arabian Sea during the last 135000 years. Palaeogeogr. Palaeoclimat. Palaeoecol. 197, 61-82.*
681 *Joeris, O., Weninger, B., 1998. Extension of the ^{14}C calibration curve to ca. 40,000 cal BC by synchronizing*
682 *Greenland $^{18}O/^{16}O$ ice core records and North Atlantic foraminifera profiles: A comparison with U/Th coral*
683 *data. Radiocarbon 40, 495-504.*
684 *Koopmann, B., 1981. Sedimentation von Saharastaub im subtropischen Nordatlantik während der letzten 25.000*
685 *Jahre. Meteor Forschungsergeb. 35, 23-59.*
686 *Lindberg, B., Berndt, C., Mienert, J., 2007. The Fugløy Reef at 70°N; acoustic signature, geologic, geomorphologic*
687 *and oceanographic setting. Int. J. Earth Sci. 96, 201-213.*
688 *Machín, F., Pelegrí, J.L., Marrero-Díaz, A., Laiz, I., Ratsimandresy, A.W., 2006. Near-surface circulation in the*
689 *southern Gulf of Cádiz. Deep-Sea Res. II 53, 1161-1181.*
690 *Mauritzen, C., Morel, J., Paillet, J., 2001. On the influence of Mediterranean water on the central waters of the*
691 *North Atlantic Ocean. Deep-Sea Res. 44, 1543-1574.*
692 *Mittelstaedt, E., 1991. The ocean boundary along the northwest African coast: Circulation and oceanographic*
693 *properties at the sea surface. Prog. Oceanogr. 26, 307-355.*
694 *Mohtadi, M., Max, L., Hebbeln, D., Baumgart, A., Krück, N., Jennerjahn, T., 2007. Modern environmental*
695 *conditions recorded in surface sediment samples off W and SW Indonesia: Planktonic foraminifera and biogenic*
696 *compounds analyses. Mar. Micropaleontol. 65, 96-112.*
697 *Moreno, A., Cacho, I., Canals, M., Prins, M.A., Sánchez-Goñi, M.-F., Grimalt, J.O., Weltje, G.J., 2002. Saharan dust*
698 *transport and high-latitude glacial climatic variability: The Alboran Sea record. Quat. Res. 58, 318-328.*
699 *Nadeau, M.J., Schleicher, M., Grootes, P., Erlenkeuser, H., Gottolong, A., Mous, D.J.W., Sarnthein, M., Willkomm,*
700 *N., 1997. The Leibniz-Labor AMS facility of the Christian-Albrechts University, Kiel, Germany. Nucl. Instrum.*
701 *Methods Phys. Res. 123, 22-30.*
702 *Ochoa, J., Bray, N.A., 1991. Water mass exchange in the Gulf of Cádiz. Deep-Sea Res. 38 (S1), 5465-5503.*

Pelegrí, J.L., Marrero-Díaz, A., Ratsimandresey, A., Antoranz, A., Cisneros-Aguirre, J., Gordo, C., Grísolia, D., Hernández-Guerra, A., Láiz, I., Martínez, A., Parrilla, G., Pérez-Rodriguez, P., Rodríguez-Santana, A., Sangrà, P., 2005. Hydrographic cruises off northwest Africa: the Canary Current and the Cape Ghir region. J. Mar. Syst. 54, 39-63.

Perez-Folgado, M., Sierro, F.J., Flores, J.A., Cacho, I., Grimalt, J.O., Zahn, R., Shackleton, N.J., 2003. Western Mediterranean planktonic foraminifera events and millennial climatic variability during the last 70 kyr. Mar. Micropaleontol. 48, 49-70.

Pflaumann, U., Sarnthein, M., Chapman, M., d'Abreu, L., Funnell, B., Huels, M., Kiefer, T., Maslin, M., Schulz, H., Swallow, J., van Kreveld, S., Vautravers, M., Vogelsang, E., Weinelt, M., 2003. Glacial North Atlantic: sea-surface conditions reconstructed by GLAMAP 2000. Paleoceanography 18, 1065.

Prins, M.A., Weltje, G.J., 1999. End-member modeling of siliciclastic grain-size distributions: the Late Quaternary record of eolian and fluvial sediment supply to the Arabian Sea and its paleoclimatic significance. In: Harbaugh, J., Watney, L., Rankey, G., Slingerland, R., Goldstein, R., Franseen, E. (Eds.), Numerical Experiments in Stratigraphy: Recent Advances in Stratigraphic and Sedimentologic Computer Simulations. SEPM, pp. 91-111.

Prins, M.A., Postma, G., Cleveringa, J., Cramp, A., Kenyon, N.H., 2000. Controls on terrigenous sediment supply to the Arabian Sea during the late Quaternary: the Indus Fan. Mar. Geol. 169, 327-349.

Ratmeyer, V., Balzer, W., Bergametti, G., Chiapello, I., Fischer, G., Wyputta, U., 1999. Seasonal impact of mineral dust on deep-ocean particle flux in the eastern subtropical Atlantic Ocean. Mar. Geol. 159, 241-252.

Reveillaud, J., Freiwald, A., Van Rooij, D., Le Guilloux, E., Altuna, A., Foubert, A., Vanreusel, A., Olu-Le Roy, K., Henriet, J.-P., 2008. The distribution of scleractinian corals in the Bay of Biscay, NE Atlantic. Facies 54, 317-331.

Roberts, J.M., Wheeler, A.J., Freiwald, A., 2006. Reefs of the deep: The biology and geology of cold-water coral ecosystems. Science 312, 543-547

Robinson, L.F., Belshaw, N.S., Henderson, G.M., 2004. U and Th concentrations and isotope ratios in modern carbonates and waters from the Bahamas. Geochim. Cosmochim. Acta 68, 1777-1789.

Robinson, L.F., Adkins, J.F., Fernandez, D.P., Burnett, D.S., Wang, S.-L., Gagnon, A.C., Krakauer, N., 2006. Primary U distribution in scleractinian corals and its implications for U series dating. Geochem. Geophysic. Geosyst. 7, Q05022, doi, 10.1029/2005GC001138.

Rogerson, M., Rohling, E.J., Weaver, P.P.E., Murray, J.W., 2004. The Azores Front since the Last Glacial Maximum. Earth Planet. Sci. Lett. 222, 779-789.

Rogerson, M., Rohling, E.J., Weaver, P.P.E., Murray, J.W., 2005. Glacial to interglacial changes in the settling depth of the Mediterranean Outflow plume. Paleoceanography 20, PA3007, doi:3010.1029/2004PA001106.

Rüggeberg, A., Dullo, W.-C., Dorschel, B., Hebbeln, D., 2007. Environmental changes and growth history of a cold-water carbonate mound (Propeller Mound, Porcupine Seabight). Int. J. Earth Sci. 96, 57-72.

Salgueiro, E., Voelker, A., Abrantes, F., Meggers, H., Pflaumann, U., Loncaric, N., González-Álvarez, R., Oliveira, P., Bartels-Jónsdóttir, H.B., Moreno, J., Wefer, G., 2008. Planktonic foraminifera from modern sediments reflect upwelling patterns off Iberia: Insights from a regional transfer function. Mar. Micropaleontol. 66, 135-164.

Sarnthein, M., Tetzlaff, G., Koopmann, B., Wolter, K., Pflaumann, U., 1981. Glacial and interglacial wind regimes over the eastern tropical Atlantic and Northwest Africa. Nature 293, 193-196.

Schiebel, R., Waniek, J., Bork, M., Hemleben, C., 2001. Planktic foraminiferal production stimulated by chlorophyll redistribution and entrainment of nutrients. Deep-Sea Res. I 48, 721-740.

Schiebel, R., Waniek, J., Zeltner, A., Alves, M., 2002. Impact of the Azores Front on the distribution of planktic foraminifers, shelled gastropods and coccolithophorids. Deep-Sea Res. II 49, 4035-4050.

Schmiedl, G., de Bovée, F., Buscail, R., Charrière, B., Hemleben, C., Medernach, L., Picon, P., 2000. Trophic control of benthic foraminiferal abundance and microhabitat in the bathyal Gulf of Lions, western Mediterranean Sea. Mar. Micropaleontol. 40, 167-188.

Scholz, D., Mangini, A., Felis, T., 2004. U-series dating of diagenetically altered fossil reef corals. Earth Planet. Sci. Lett. 218, 163-178.

Schönfeld, J., Zahn, R., 2000. Late Glacial to Holocene history of the Mediterranean Outflow. Evidence from benthic foraminiferal assemblages and stable isotopes at the Portuguese margin. Palaeogeogr. Palaeoclimat. Palaeoecol. 159, 85-111.

Schröder-Ritzrau, A., Freiwald, A., Mangini, A., 2005. U/Th-dating of deep-water corals from the eastern North Atlantic and the western Mediterranean Sea. In: Freiwald, A., Roberts, J.M. (Eds.), Cold-water Corals and Ecosystems. Springer, Heidelberg, pp. 691-700.

Sierro, F.J., Flores, J.A., Baraza, J., 1999. Late glacial to recent paleoenvironmental changes in the Gulf of Cadiz and formation of sandy contourite layers. Mar. Geol. 155, 157-172.

Somoza, L., Diaz-del-Rio, V., Leon, R., Ivanov, M., Fernandez-Puga, M.C., Gardner, J.M., Hernandez-Molina, F.J., Pinheiro, L.M., Rodero, J., Lobato, A., 2003. Seabed morphology and hydrocarbon seepage in the Gulf of Cádiz mud volcano area: Acoustic imagery, multibeam and ultra-high resolution seismic data. Mar. Geol. 195, 153-176.

Stirling, C.H., Esat, T.M., Lambeck, K., McCulloch, M.T., 1998. Timing and duration of the Last Interglacial: evidence for a restricted interval of widespread coral reef growth. Earth Planet. Sci. Lett. 160, 745-762.

Stoll, H.M., Arevalos, A., Burke, A., Ziveri, P., Mortyn, G., Shimizu, N., Unger, D., 2007. Seasonal cycles in biogenic production and export in Northern Bay of Bengal sediment traps. Deep-Sea Res. II 54, 558-580.

766 *Stuut, J.-B.W., Prins, M.A., Schneider, R.R., Weltje, G.J., Jansen, J.H.F., Postma, G., 2002. A 300-kyr record of*
767 *aridity and wind strength in southwestern Africa: inferences from grain-size distributions of sediments on*
768 *Walvis Ridge, SE Atlantic. Mar. Geol. 180, 221-233.*
769 *Stuut, J.B., Zabel, M., Ratmeyer, V.H., P., Schefuß, E., Lavik, G., Schneider, R.R., 2005. Provenance of present-day*
770 *eolian dust collected off NW Africa: implications for deep-marine sediment studies. J. Geophys. Res. 110,*
771 *D04202.*
772 *Taviani, M., Bouchet, P., Metivier, B., Fontugne, M., Delibrias, G., 1991. Intermediate steps of southwards faunal*
773 *shifts testified by last glacial submerged thanatocoenoses in the Atlantic Ocean. Palaeogeography,*
774 *Palaeoclimatology, Palaeocology 86, 331-338.*
775 *Taviani, M., Remia, A., Corselli, C., Freiwald, A., Malinverno, E., Mastrototaro, F., Savini, A., Tursi, A., 2005. First*
776 *geo-marine survey of living cold-water Lophelia reefs in the Ionian Sea (Mediterranean basin). Facies 50, 409-*
777 *417.*
778 *Thiel, H., Pfannkuche, O., Schriever, G., Lochte, K., Gooday, A.J., Hemleben, C., Mantoura, R.F.C., Turley, C.M.,*
779 *Patching, J.W., Riemann, F., 1989. Phytodetritus on the deep-sea floor in a central region of the Northeast*
780 *Atlantic. Biol. Oceanogr. 6, 203-239.*
781 *Thompson, W.G., Spiegelman, M.W., Goldstein, S.L., Speed, R.C., 2003. An open-system model for U-series age*
782 *determinations of fossil corals. Earth Planet. Sci. Lett. 210, 365-381.*
783 *Thunell, R., Reynolds, L., 1984. Sedimentation of planktonic foraminifera: Seasonal changes in species flux in the*
784 *Panama Basin. Micropaleontology 30, 243-262.*
785 *Tyler, B., Amaro, T., Arzola, R., Cunha, M.R., De Stigter, H., Gooday, A., Huvenne, V., Ingels, J., Kiriakoulakis, K.,*
786 *Lastras, G., Masson, D.G., Oliveira, A., Pattenden, A., Vanreusel, A., Van Weering, T.C.E., Vitorino, J., Witte, U.,*
787 *Wolff, G., 2009. Europe's Grand Canyon: Nazaré Submarine Canyon. Oceanography 22, 46-57.*
788 *Tyler, P.A., Harvey, R., Giles, L.A., Gage, J.D., 1992. Reproductive strategies and diet in deep-sea nuculanid*
789 *protobranchs (Bivalvia: Nuculoidea) from the Rockall Trough. Mar. Biol. 114, 571-580.*
790 *Voelker, A.H.L., Lebreiro, S.M., Schönfeld, J., Cacho, I., Erlenkeuser, H., Abrantes, F., 2006. Mediterranean*
791 *outflow strengthening during northern hemisphere coolings: A salt source for the glacial Atlantic. Earth Planet.*
792 *Sci. Lett. 245, 39-55.*
793 *Waller, R.G., Tyler, P.A., 2005. The reproductive biology of two deep-water, reef-building scleractinians from the*
794 *NE Atlantic Ocean. Coral Reefs 24, 514-522.*
795 *Weltje, G., 1997. End-member modeling of compositional data: Numerical-statistical algorithms for solving the*
796 *explicit mixing problem. Math. Geol. 29, 503-549.*
797 *Wheeler, A.J., Beyer, A., Freiwald, A., de Haas, H., Huvenne, V., Kozachenko, M., Olu-Le Roy, K., Opderbecke, J.,*
798 *2007. Morphology and environment of cold-water coral carbonate mounds on the NW European margin. Int. J.*
799 *Earth Sci. 96, 37-56.*
800 *White, M., Mohn, C., de Stigter, H., Mottram, G., 2005. Deep-water coral development as a function of*
801 *hydrodynamics and surface productivity around the submarine banks of the Rockall Trough, NE Atlantic. In:*
802 *Freiwald, A., Roberts, J.M. (Eds.), Cold-Water Corals and Ecosystems. Springer, Heidelberg, pp. 503-514.*
803 *White, M., Roberts, J.M., van Weering, T.C.E., 2007. Do bottom-intensified diurnal tidal currents shape the*
804 *alignment of carbonate mounds in the NE Atlantic? Geo-Mar. Lett. 27, 391-397.*
805 *Wienberg, C., Hebbeln, D., Fink, H.G., Mienis, F., Dorschel, B., Vertino, A., López Correa, M., Freiwald, A., 2009.*
806 *Scleractinian cold-water corals in the Gulf of Cádiz - first clues about their spatial and temporal distribution.*
807 *Deep-Sea Res. I 56, 1873-1893.*
808 *Wilke, I., Meggers, H., Bickert, T., 2009. Depth habitats and seasonal distributions of recent planktic foraminifers*
809 *in the Canary Islands region (29°N) based on oxygen isotopes. Deep-Sea Res. I 56, 89-106.*
810
811
812

Figure 1. Map of the Gulf of Cádiz (GoC) showing the coring sites (bathymetric data source: GEBCO). Reference sediment core GeoB 9064 (black triangle) and coral-bearing sediment cores (A-D). A: Hespérides mud volcano (GeoB 9018), B: Faro mud volcano (GeoB 9031, GeoB 9032), C: Renard Ridge (GeoB 9070, GeoB 12101, GeoB 12102, GeoB 12103, GeoB 12104, M2004-02), D: north of Meknes mud volcano (GeoB 12106). Indicated are the reported occurrences of fossil cold-water corals (after Wienberg et al., 2009). Lower left: photographs showing characteristic 'coral graveyards' in the southern GoC, Moroccan margin (position is indicated on the map as p1, p2) (images ©MARUM, Bremen).

Figure 2. **Initial U-isotopic ratios of cold-water corals (lower graph) and ^{232}Th concentration (upper graph).** δ^{234}U is in almost all cases very close to present-day seawater (149.9‰: blue dashed line; range of 149.9±10‰: light blue bar), except for the deepest sample in core GeoB 12104 (+38‰). ^{232}Th concentrations for 75% of all samples are below 10 ng g^{-1} (green dashed line).

Figure 3. ^{230}Th/U datings conducted on cold-water coral fragments collected in the GoC. AMS ^{14}C ages presented by Wienberg et al. (2009) are implemented. Note that solely reef-forming species such as *Madrepora oculata* and *Lophelia pertusa* are considered showing that >90% of all coral ages coincide with glacial periods. Marine Isotope Stages (MIS) are indicated by grey bars based on SPECMAP δ^{18}O stack (Imbrie et al. 1989).

Figure 4. Multi-proxy data of sediment core GeoB 9064. (**a**) Estimated sedimentation rate, (**b**) stable oxygen isotopes record (lower curve) compared with the GRIP ice core record (upper curve) (**c**) median grain size (terrigenous and bulk sediment), (**d**) relative aeolian input, (**e**) relative wind strength, and (**f**) productivity index based on the ratio of high- to low-productivity planktonic foraminiferal assemblages. AMS ^{14}C dates obtained for core GeoB 9064 are marked by black diamonds. For comparison, U/Th (squares; this study) and AMS ^{14}C coral dates (triangles; Wienberg et al., 2009) obtained for the past 50 kyr are

implemented. Note that solely reef-forming species such as *Madrepora oculata* and *Lophelia pertusa* are considered.

Figure 5. The $\delta^{18}O$ record and planktonic foraminiferal abundance for sediment core GeoB 9064. (**a**) $\delta^{18}O_{N.\ pachyderma\ (dex.)}$, (**b**) *Neogloboquadrina pachyderma* (black: dex., grey: sin.), (**c**) *Globigerinita glutinata*, (**d**) *Globigerina bulloides*, (**e**) *Globigerinoides ruber* (black) and *Globigerinoides sacculifer* (grey), (**f**) *Globorotalia inflata*, (**g**) *Globorotalia scitula*. Younger Dryas (YD) and Marine Isotope Stages (MIS) 2 and 3 are indicated.

Figure1

Click here to download high resolution image

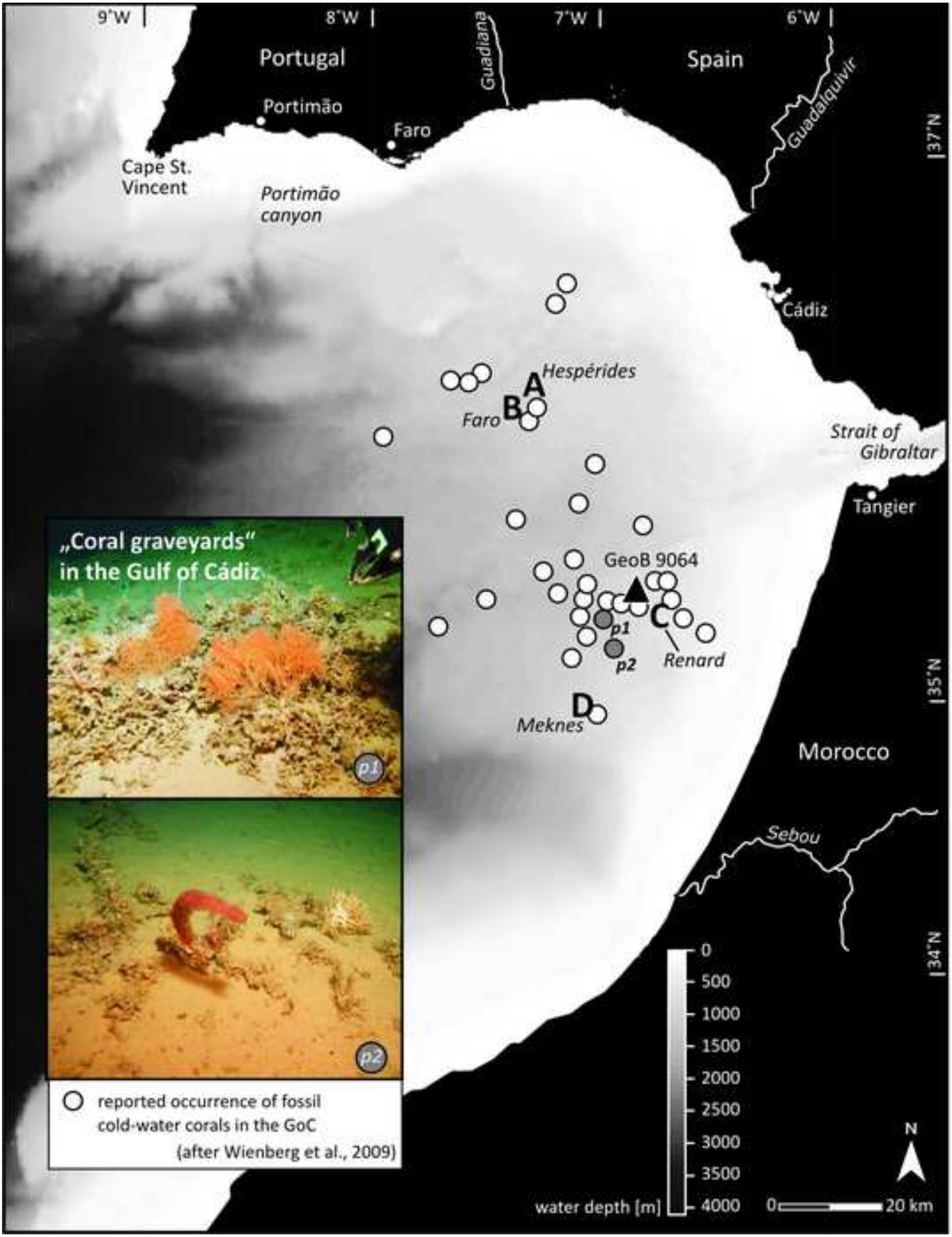

Figure2

Click here to download high resolution image

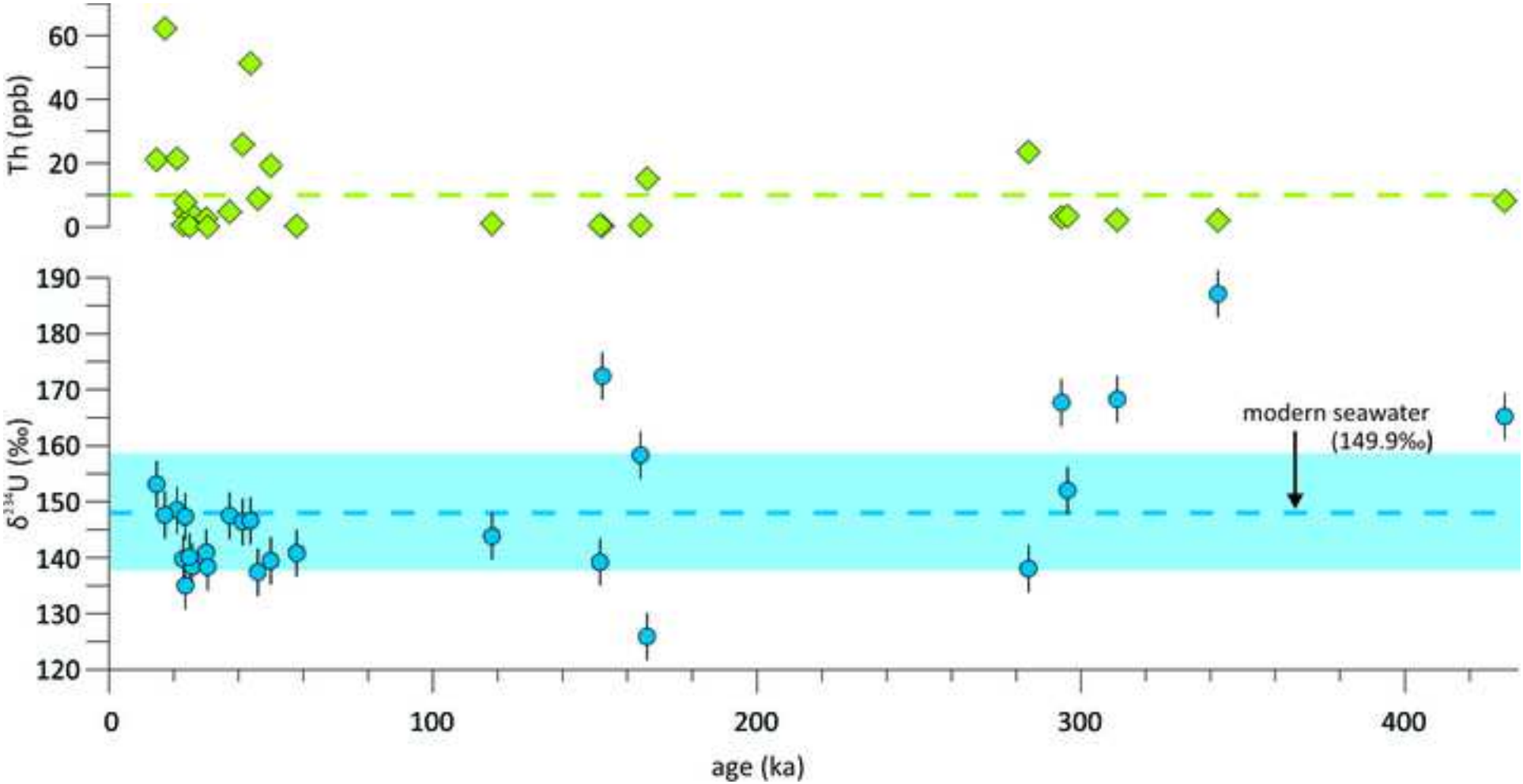

Figure3

Click here to download high resolution image

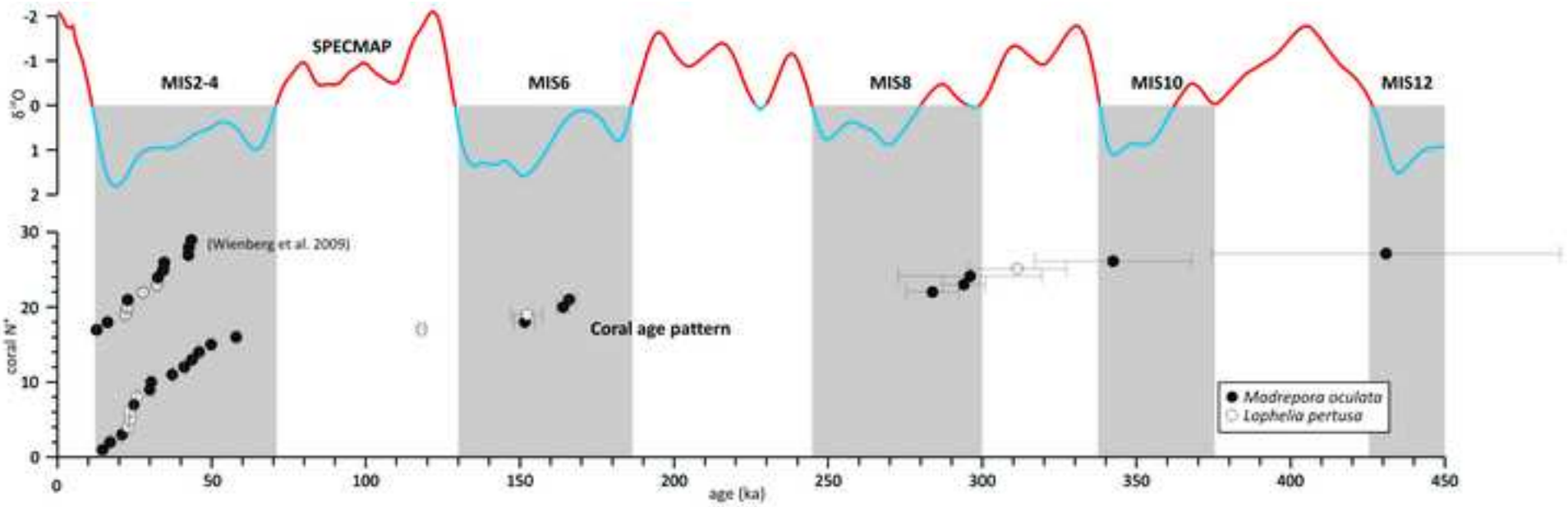

Figure4

Click here to download high resolution image

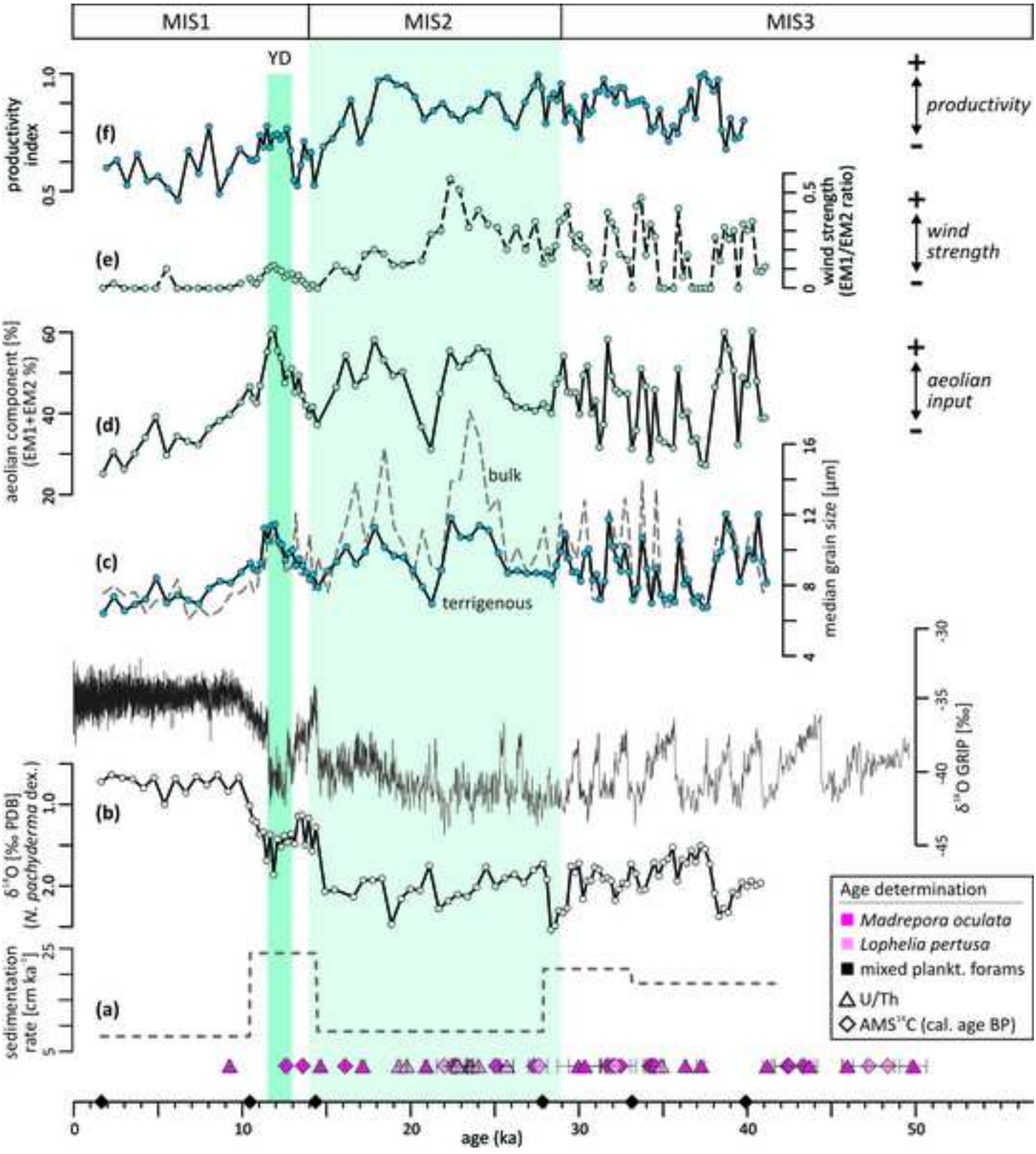

Figure5

Click here to download high resolution image

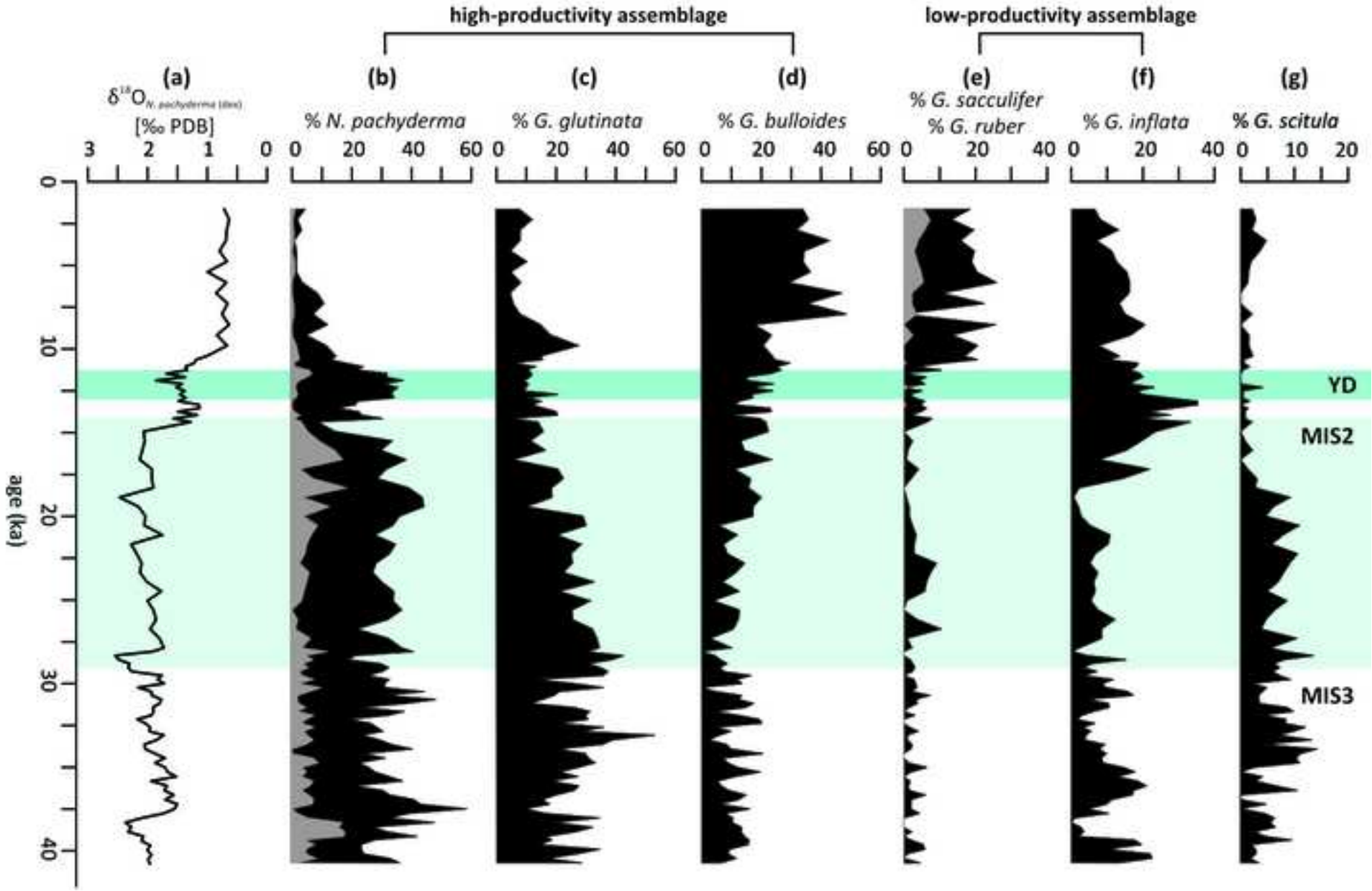

Table

Click here to download Table: Wienberg et al_tables_1st revision.doc

Table 1. Metadata of coral-bearing sediment cores collected from various sites in the Gulf of Cádiz (indicated in Figure 1 as A, B, C, D). Abbreviations: Lat, latitude; Lon, longitude; Wd, water depth; Rec, recovery; Mv, mud volcano; Cm, coral mound; SM, Spanish margin; MM, Moroccan margin; R, Ridge; PDE, Pen Duick Escarpment; Mo, *Madrepora oculata*; Lp, *Lophelia pertusa*. Cruises: 1, RV *Sonne* cruise SO175; 2, RV *Maria S. Merian* MSM01-3; 3, RV *Pelagia* cruise 64PE229.

			Cruise	Location	Core-ID	Lat (°N)	Lon (°W)	Wd (m)	Rec (cm)	Coral content
A	Mv	SM	1	Hespérides Mv	GeoB 9018	36°10.98’	07°18.37'	702	347	0-5 cm: dendrophylliids, 5-347 cm: solely Mo; strongly altered fragments.
B	Mv	SM	1	Faro Mv (lower flank)	GeoB 9031	36°05.75’	07°23.28’	897	484	0-160 cm: Mo-dominated; strongly altered fragments.
	Mv	SM	1	Faro Mv (top)	GeoB 9032	36°05.55'	07°23.57'	843	220	0-60 cm: Mo-dominated, 60-220 cm: mud breccia.
C	Cm	MM	1	W Renard R	GeoB 9070	35°22.00’	06°51.90’	594	560*	0-560 cm: Mo and Lp.
	Cm	MM	2	W Renard R	GeoB 12104	35°21.99'	06°51.90'	590	523	0-523 cm: Mo and Lp
	Cm	MM	2	Renard R	GeoB 12102	35°21.11'	06°50.96'	585	518	0-518 cm: Mo, Lp, and dendrophylliids.
	Cm	MM	2	Renard R	GeoB 12103	35°21.18'	06°50.90'	591	568	0-568 cm: Mo and Lp.
	Cm	MM	2	PDE	GeoB 12101	35°18.88'	06°48.08'	545	468	0-468 cm: Mo, Lp, and dendrophylliids.
	Cm	MM	3	PDE	M2004-02	35°17.68'	06°47.25'	523	861	0-861 cm: Mo, Lp, and dendrophylliids.
D	Cm	MM	2	N of Meknes Mv	GeoB 12106	34°59.49'	07°04.56'	758	303	30-303 cm: Mo and Lp.

* the uppermost 40 cm of core GeoB 9070 were disturbed due to coring operation, thus the undisturbed core depth ranges from 40 to 600 cm

Table 2. Ages, isotope concentrations and ratios (n.a., not available).

N°	Sample ID	Depth (cm)	Coral	Labcode	Age (ka)	± (ka)	^{238}U (ppm)	± (ppm)	^{232}Th (ppb)	± (ppb)	δ^{234}U(M) (‰)	± (‰)	δ^{234}U(0) (‰)	± (‰)
	1	*2*	*3*	*4*	*5*		*6*		*7*		*8*		*9*	
01	GeoB 9018	3	Mo	n.a.	**14.65**	0.09	4.020	0.004	21.019	0.052	149.8	1.9	156.1	2.0
02	GeoB 9018	123	Mo	n.a.	**294.00**	7.00	4.329	0.004	3.021	0.006	73.1	1.4	167.7	3.3
03	GeoB 9018	272	Mo	n.a.	**283.80**	8.50	4.005	0.004	23.536	0.064	61.9	1.5	138.0	3.3
04	GeoB 9031	10	Mo	n.a.	**20.92**	0.12	4.956	0.005	21.400	0.055	139.9	1.8	148.5	1.9
05	GeoB 9031	93	Mo	n.a.	**37.25**	0.23	5.263	0.007	4.796	0.009	132.8	2.3	147.5	2.5
06	GeoB 9031	150	Mo	n.a.	**45.94**	0.33	4.338	0.004	8.875	0.016	120.6	1.4	137.4	1.6
07	GeoB 9032	20	Mo	n.a.	**17.15**	0.15	4.447	0.005	62.092	0.192	140.6	1.6	147.6	1.7
08	GeoB 9032	47	Mo	n.a.	**41.17**	0.25	4.512	0.005	25.841	0.070	130.3	1.8	146.4	2.0
09	GeoB 9070	47	Lp	n.a.	**23.50**	0.12	4.622	0.003	4.428	0.010	137.9	1.1	147.3	1.2
10	GeoB 9070	298	Mo	n.a.	**43.68**	0.28	3.552	0.003	51.216	0.079	129.6	1.8	146.6	2.0
11	GeoB 9070	520	Mo	n.a.	**166.00**	2.40	3.968	0.004	15.089	0.033	78.7	1.7	125.9	2.7
12	GeoB 12101	57	Mo	Gif-1525	*not dateable*		3.085	0.004	0.351	0.002	59.5	3.2	/	/
13	GeoB 12101	146	Lp	Gif-1389	*not dateable*		3.214	0.004	0.920	0.003	47.4	3.0	/	/
14	GeoB 12101	451	Mo	Gif-1527	**430.76**	56.55	2.589	0.002	8.092	0.026	48.9	3.3	165.2	3.3
15	GeoB 12102	28	Mo	Gif-1529	**57.96**	0.74	4.390	0.005	0.316	0.001	119.5	2.7	140.8	2.7
16	GeoB 12102	166	Lp	Gif-1528	**118.16**	1.10	4.220	0.003	1.075	0.003	103.0	1.9	143.8	1.9
17	GeoB 12102	238	Lp	Gif-1390	**152.27**	5.12	3.035	0.003	0.306	0.003	112.1	2.9	172.4	2.9
18	GeoB 12102	376	Mo	Gif-1388	**151.56**	3.37	3.614	0.003	0.491	0.002	90.7	3.0	139.2	3.0
19	GeoB 12102	493	Mo	Gif-1386	**164.02**	2.01	3.194	0.003	0.495	0.002	99.5	1.8	158.3	1.8
20	GeoB 12103	34	Lp	Gif-1530	**22.88**	0.38	3.881	0.004	0.636	0.003	131.0	2.0	139.8	2.0
21	GeoB 12103	88	Lp	Gif-1392	**25.72**	0.39	4.462	0.006	3.873	0.010	128.7	2.9	138.4	2.9
22	GeoB 12103	200	Mo	Gif-1531	**29.98**	1.26	3.610	0.004	2.644	0.011	129.4	3.3	140.9	3.3
23	GeoB 12103	317	Mo	Gif-1532	**30.43**	0.96	3.828	0.004	0.192	0.003	126.9	2.2	138.3	2.2
24	GeoB 12103	444	Mo	Gif-1533	**49.85**	0.80	3.693	0.005	19.205	0.071	121.1	2.4	139.4	2.4
25	GeoB 12104	8	Lp	Gif-1387	**23.57**	0.18	4.435	0.003	7.778	0.016	126.3	1.7	135.0	1.7
26	GeoB 12104	373	Lp	Gif-1534	**311.20**	15.74	3.658	0.003	2.161	0.012	69.8	2.2	168.3	2.2
27	GeoB 12104	491	Mo	Gif-1535	**342.29**	25.38	3.492	0.004	2.003	0.008	71.1	2.6	187.1	2.6
28	GeoB 12106	117	Mo	Gif-1391	**295.86**	23.27	3.421	0.004	3.421	0.004	65.9	2.8	152.0	2.8
29	M2004-02	49	Mo	Gif-1631	**9.15**	0.71	3.512	0.011	0.103	0.014	149.3	3.0	153.2	3.0
30	M2004-02	85	Lp	Gif-1632	**19.36**	0.54	3.943	0.007	0.625	0.008	138.8	2.5	146.6	2.5
31	M2004-02	105	Lp	Gif-1633	**19.87**	0.52	3.284	0.010	0.695	0.006	136.0	3.9	143.9	3.9
32	M2004-02	141	Lp	Gif-1634	**21.37**	0.42	3.862	0.007	4.666	0.013	136.5	2.3	145.0	2.3
33	M2004-02	147	Lp	Gif-1635	**22.75**	0.26	4.016	0.006	2.209	0.006	133.0	2.9	141.8	2.9
34	M2004-02	176	Lp	Gif-1636	**24.03**	0.26	3.921	0.008	11.534	0.031	131.4	3.3	140.6	3.3
35	M2004-02	247	Lp	Gif-1637	**34.90**	0.43	3.099	0.004	0.310	0.001	130.3	2.5	143.8	2.5
36	M2004-02	273	Mo	Gif-1638	**36.27**	0.43	3.804	0.008	3.049	0.008	124.5	1.6	138.0	1.6
37	M2004-02	313	Lp	Gif-1639	**142.08**	1.92	4.068	0.010	2.908	0.009	96.6	2.3	144.4	2.4
38	M2004-02	343	Lp	Gif-1640	**175.01**	2.79	3.846	0.005	14.820	0.026	85.3	2.5	139.9	2.5
39	M2004-02	363	Mo	Gif-1641	**242.07**	8.35	3.174	0.008	0.506	0.003	85.4	2.7	169.3	2.7
40	M2004-02	403	Lp	Gif-1642	**262.80**	7.46	3.126	0.007	3.116	0.007	74.2	2.9	155.9	2.9

NOTE: ***Column 1****: S*ample label. ***Column 2****:* Depth in core. ***Column 3***: Reef-forming scleractinian cold-water coral species, Lp *Lophelia pertusa*, Mo *Madrepora oculata*. ***Column 4***: Labcode (not available for datings conducted at IFM-GEOMAR, N° 1-11). ***Column 5***: Calculated coral ages. ***Column 6***: ^{238}U concentration. ***Column 7***: ^{232}Th concentration. ***Column 8***: Measured ^{234}U/^{238}U activity ratios (δ^{234}U(M)) are presented as deviation per mil (‰) from the equilibrium value. ***Column 9***: Decay corrected ^{234}U/^{238}U activity ratios (δ^{234}U(0)) are calculated from the given ages and with λ_{234U}: 2.8263x10^{-6} yr^{-1}. Note that ages are strictly reliable having values between 146.6‰ and 149.6‰ (modern seawater), reliable with values of 149±10‰, unreliable with values >149±10‰ (see also Stirling et al., 1998; Robinson et al., 2004; Esat and Yokoyama, 2006).

Table 3. AMS ^{14}C dates determined on multi-species samples of planktonic foraminifera from sediment core GeoB 9064. The AMS ^{14}C ages were corrected for ^{13}C and a mean ocean reservoir age of 400 years, and were converted to calendar years using the CALPAL 2007 Hulu software. Estimated sedimentation rates for core GeoB 9064 are supplemented.

Core depth (cm)	**Labcode**	**Conventional age** ^{14}C **age** (years)	± error	**CALPAL age** 1σ (68%) (calendar years B.P., P.=AD 1950)	± error	**Sedimentation rate** (cm kyr^{-1})
GeoB 9064						
4	Poz-20282	2 095	30	1 630	50	-
74	KIA-10065	9 665	60	10 430	100	7.95
169	KIA-13060	12 660	80	14 370	240	24.11
289	KIA-23840	23 440	180	27 860	190	8.90
399	KIA-29420	29 020	320	33 090	420	21.03
524	KIA-35660	35 260	630	39 960	960	18.20